# Studies on the Reactions of Dihydrogen with Salts of Platinum Carbonyl Cluster Anions (Chini Clusters) and Redox Active Countercations

Sumit Bhaduri,*,† Nalinava Sen Gupta,‡ Goutam Kumar Lahiri,*,‡ and Pradeep Mathur*,‡

*Reliance Industries Limited, V. N. Purav Marg, Chembur, Bombay 400 071, India, and Chemistry Department, Indian Institute of Technology—Bombay, Bombay 400076, India*

*Received March 7, 2004*

Reactions of $A_n[Pt_{12}(CO)_{24}]$ (A = methylene blue ($MB^+$), safranine O ($Saf^+$), nicotinamide benzyl chloride ($BNA^+$), $n = 2$; A = methylviologen ($MV^{2+}$), $n = 1$) with dihydrogen in DMF and DMSO have been studied. Spectroscopic (NMR, ESR, and UV−vis) monitoring shows selective and total reduction of $MB^+$, $Saf^+$, and $MV^{2+}$ to MBH, SafH, and $MV^{+\cdot}$ respectively, accompanied by conversion of $[Pt_{12}(CO)_{24}]^{2-}$ to $[Pt_9(CO)_{18}]^{2-}$. No BNAH (analogue and model for NADH) is formed in the reaction of $[BNA]_2[Pt_{12}(CO)_{24}]$ with dihydrogen. However, in the reactions of $BNA^+Cl^-$, $[Saf]_2[Pt_{12}(CO)_{24}]$, and dihydrogen, BNAH is formed in small quantities in DMSO and quantitatively in a biphasic system (water and dichloromethane). The redox behaviors of $MB^+$, $Saf^+$, $MV^{2+}$, and $BNA^+$ as chloride salts have also been studied in DMF by cyclic voltammetry, and the data have been used to rationalize some of the observed reactions. The dihydrogen-driven, $[Bu_4N]_2[Pt_{12}(CO)_{24}]$-catalyzed transport of $A^+$ ($A^+ = MB^+$, $Saf^+$) as AH through a liquid membrane has also been studied.



## Introduction

Platinum carbonyl clusters of the general formula $[Pt_3(CO)_6]_n^{2-}$ ($n = 3-6$), commonly known as Chini clusters, have unique redox properties. As specially prepared platinum colloids, these clusters can equilibrate with dihydrogen and protons[1] according to reaction a.

$$(n-1)[Pt_3(CO)_6]_n^{2-} + H_2 \rightleftarrows n[Pt_3(CO)_6]_{n-1}^{2-} + 2H^+ \quad (a)$$
$$n = 4-6$$

We have reported mechanistic investigations on these reactions, which are accompanied by spectacular color changes and clean isosbesticities in the UV−visible spectra.[2] Several years ago we had also reported the use of Chini clusters as redox catalysts in the reduction of *p*-quinone to 1,4-dihydroxybenzene by dihydrogen.[3] Subsequently we had communicated preliminary results on the use of these clusters as *catalysts* in pH-driven electron transport across a *liquid membrane* as well as in dihydrogen-driven reduction of $NAD^+$ (nicotinamide adenine dinucleotide).[4]

Selective reduction of $NAD^+$ to NADH by dihydrogen with an organometallic catalyst is an important research target,[5] as such a reaction, in combination with NADH-dependent enzymes, enables the enantioselective syntheses of chiral amino acids or L-lactate.[5a,b] To effect the latter reaction in a biphasic reaction medium, i.e., a reaction medium consisting of water and a water-immiscible organic solvent, we used the redox-active dye SafranineO ($Saf^+$) as a *shuttle carrier*.[4a] Such a carrier had to be used, as $NAD^+$ is insoluble in organic solvents while $[Pt_3(CO)_6]_n^{2-}$ clusters are insoluble and unstable in water. Also, the direct hydrogen-driven reduction of $NAD^+$, catalyzed by Sephadex-supported Chini clusters, had been found to be exceedingly slow.[4b] The reduced shuttle carrier, due to its solubility in both solvents, is capable of transporting one proton and two electrons across the phase boundary of the two liquids according to reactions b−d.

$$3[Pt_{12}(CO)_{24}]^{2-} + H_2 \rightarrow 4[Pt_9(CO)_{18}]^{2-} + 2H^+ \quad (b)$$

$$Saf^+ + H^+ + 4[Pt_9(CO)_{18}]^{2-} \rightarrow 3[Pt_{12}(CO)_{24}]^{2-} + SafH \quad (c)$$

$$SafH + NAD^+ \rightarrow Saf^+ + NADH \quad (d)$$

The work presented here has been carried out with the following objectives. First, to present detailed results on reaction c and to explore the feasibility of similar

* To whom correspondence should be addressed. E-mail: mathur@iitb.ac.in (P.M.).
† Reliance Industries Limited.
‡ Indian Institute of Technology—Bombay.

(1) (a) Longoni, G.; Chini, P. *J. Am. Chem. Soc.* **1976**, *98*, 7225. (b) Calabrese, J. C.; Dahl, L. F.; Chini, P.; Longoni, G.; Martinengo, S. *J. Am. Chem. Soc.* **1974**, *96*, 2614. (c) Thanos, I.; Simon, H. *Angew. Chem., Int. Ed. Engl.* **1986**, *25*, 462.

(2) Bhaduri, S.; Lahiri, G. K.; Paul, H.; Mukesh, D. *Organometallics* **2001**, *20*, 3329.

(3) (a) Basu, A.; Bhaduri, S.; Sharma, K. R. *J. Chem. Soc., Dalton Trans.* **1984**, 2315. (b) Bhaduri, S.; Sharma, K. R. *J. Chem. Soc., Chem. Commun.* **1992**, 1593. (c) Bhaduri, S.; Sharma, K. R. *J. Chem. Soc., Chem. Commun.* **1996**, 207.

(4) (a) Bhaduri, S.; Mathur, P.; Payra, P.; Sharma, K. *J. Am. Chem. Soc.* **1998**, *120*, 12127. (b) Bhaduri, S. *Curr. Sci.* **2001**, 1378.

10.1021/om049833e CCC: $27.50 
Publication on Web 06/19/2004

**Scheme 1**

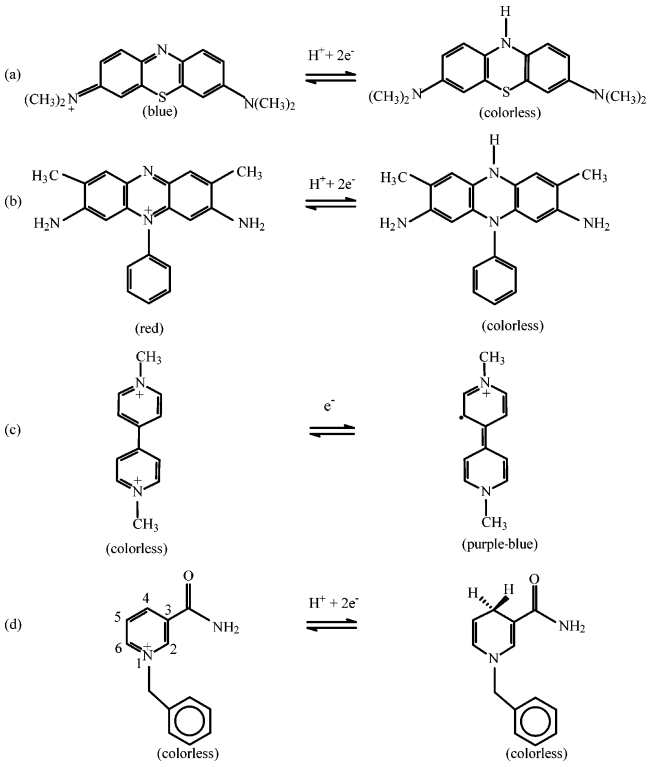


reactions with other redox-active cations. This is important, since the ultimate goal is to find effective shuttle carriers for a wide variety of redox reactions. The designations of these salts used for this purpose and the structural formulas of the countercations $A^{n+}$ ($n = 1, 2$) in both the oxidized and reduced states are shown in Scheme 1. It may be noted that $BNA^+$ is a well-accepted model[6] for biological $NAD^+$. Also, in the presence of protons, $MB^+$, $Saf^+$, and $BNA^+$ are all one-proton, two-electron acceptors. In contrast, $MV^{2+}$ is a well-established proton-independent one-electron acceptor.

Second, we wanted to study and confirm that the cluster-catalyzed reductions of $A^{n+}$ are fully *chemo- and regioselective*. Overreduction and/or partial degradation of $A^{n+}$ during the hydrogen-driven reduction process is always a possibility. The disappearance of the characteristic colors of $MB^+$ and $Saf^+$ on reduction is commonly taken to be indicative of the formation of MBH and SafH. However, overreduction and/or degradation of $MB^+$ and $Saf^+$ also brings about bleaching. Similarly, borohydride reduction of $BNA^+$ is known to give both 2- and 4-reduced products.[6] In fact sodium dithionite, a reducing agent used more than 50 years ago, is still the only reducing agent that is known to give selective hydride addition in the 4-position[6c] of $NAD^+$ or $BNA^+$.

To attain the objectives mentioned above, we have studied the reactions of $[MB]_2[Pt_{12}(CO)_{24}]$ (**1**), $[Saf]_2[Pt_{12}(CO)_{24}]$ (**2**), $[MV][Pt_{12}(CO)_{24}]$ (**3**), and $[BNA]_2[Pt_{12}(CO)_{24}]$ (**4**) (Scheme 1) with dihydrogen in *organic solvents* and monitored the reactions spectroscopically (NMR, ESR, IR, and UV−vis). We have also carried out cyclic voltammetric studies on chloride salts of $A^{n+}$ in dimethylformamide (DMF) to explore their redox characteristics in the absence of protons. The spectroscopic and electrochemical studies have enabled us to establish the occurrence and selectivity of the reductions and the extent to which thermodynamic parameters influence these reactions.

Finally, *shuttle carriers* are known to adopt a variety of mechanisms for the transport of electrons, protons, cofactors, etc. across the biological membranes.[7] In view of this, we have also studied the transport of $MB^+$ and $Saf^+$ in a model system. In the model *liquid membrane*, a dichloromethane layer separates two water layers, one of which contains either $MB^+Cl^-$ or $Saf^+Cl^-$. In the presence of dihydrogen, $[Pt_{12}(CO)_{24}]^{2-}$ catalyzes the transport of $MB^+$ and $Saf^+$ as MBH and SafH, respectively, from one aqueous layer to the other.

## Results and Discussion

**(a) Syntheses and Characterizations of 1−4.** A methanolic solution of the sodium salt of $[Pt_{12}(CO)_{24}]^{2-}$ is prepared according to the procedure reported by Chini and Longoni.[1] On addition of concentrated solutions of ACl ($A = Saf^+$, $MB^+$, $BNA^+$) or $ACl_2$ ($A = MV^{2+}$) the salts **1**−**4** precipitate out. They have been characterized on the basis of IR, NMR ($^1H$), and analytical (C, H, N) data (see the Experimental Section). All of the salts are soluble in DMF and DMSO, and **1** and **2** are also soluble to a lesser extent in ethyl acetate, dichloromethane, and chloroform. Attempts were also made to synthesize $A_n[Pt_9(CO)_{18}]$ ($A = Saf^+$, $MB^+$ $n = 2$; $A = MV^{2+}$, $n = 1$) analogues. However, in all the cases $A_n[Pt_{12}(CO)_{24}]$ precipitated out. This indicates favorable thermodynamics for the oxidation of $[Pt_9(CO)_{18}]^{2-}$ to $[Pt_{12}(CO)_{24}]^{2-}$ by the cations in protic media.

The IR spectra of **1**−**4** have been recorded and compared with that of $[NBu_4]_2[Pt_{12}(CO)_{24}]$. They all have the characteristic $\nu_{CO}$ signals (KBr disk) of $[Pt_{12}(CO)_{24}]^{2-}$ at 2045 (s) and 1870 (m) $cm^{-1}$. In solution (dichloromethane) similar IR spectra are obtained but the bridging carbonyl is weaker than what is observed in KBr. The $^1H$ NMR spectra of **2**−**4** are identical with that of the respective ACl or $ACl_2$. The NMR spectrum of **1,** interestingly, is an exception, in that the signals are very weak and featureless. The explanation for this is discussed later. In the UV−visible spectra of **1** and **2**, the characteristic band of $[Pt_{12}(CO)_{24}]^{2-}$ at 620 nm ($\epsilon =$ 23 000) is masked by the much stronger absorption

(5) (a) Delecouls-Servat, K.; Basseguy, R.; Bergel, A. *Chem. Eng. Sci.* **2002**, 57, 4633. (b) Stephen, C. S. *Chem. Eng. News* **2000**, *78*, 59. (c) Wong, C. H.; Daniels, L.; Orme-Johnson, W. H.; Whitesides, G. M. *J. Am. Chem. Soc.* **1981**, *103*, 6227. (d) Chao, S.; Wrighton, M. S. *J. Am. Chem. Soc.* **1987**, *109*, 5886. (e) Abril, O.; Whitesides, G. M. *J. Am. Chem. Soc.* **1982**, *104*, 1552. (f) Chen, C. S.; Sih, C. J. *Angew. Chem., Int. Ed. Engl.* **1989**, *28*, 695. (g) Steckhan, E.; Herrmann, S.; Ruppert, R.; Dietz, E.; Frede, M.; Spika, E. *Organometallics* **1991**, *10*, 1568. (h) Jang, S.-H.; Kang, H.-Y.; Kim, G.-J.; Seo, J.-H.; Ryu, Y.-W. *J. Microbiol. Biotechnol.* **2003**, *13*, 501. (i) Hollmann, F.; Schmid, A.; Steckhan, E. *Angew. Chem., Int. Ed.* **2001**, *40*, 169. (j) Stengelin, M.; Patel, R. N. *Biocatal. Biotrans.* **2000**, *18*, 373. (k) Slatner, M.; Nagl, G.; Haltrich, D.; Kulbe, K. D.; Nidetzky, B. *Biocatal. Biotrans.* **1998**, *16*, 351. (l) Torres, R. A.; Schiott, B.; Bruice, T, C. *J. Am. Chem. Soc.* **1999**, *121*, 8164. (m) Bradshaw, C. W.; Wong, C. H.; Hummel, W.; Kula, M. R. *Bioorg. Chem.* **1991**, *19*, 29.

(6) Gase, R. A.; Boxhon, G.; Pandit, U. K. *Tetrahedron Lett.* **1976**, 2889. (b) Roberts, R. M. G.; Ostovic, D.; Kreevoy, M. M. *J. Org. Chem.* **1983**, *48*, 2053. (c) Mauzerall, D.; Westheimer, F. H. *J. Am. Chem. Soc.* **1965**, *77*, 2261. (d) Willner, I.; Maidan, R.; Shapira, M. *J. Chem. Soc, Perkin Trans. 2* **1990**, *4*, 559. (e) Oae, S.; Nagata, T.; Yoshimura, T.; Fujimori, K. *Tetrahedron Lett.* **1982**, *23*, 3189. (f) Bunting, J. W.; Sindhuatmadja, S. *J. Org. Chem.* **1981**, *46*, 4211.

(7) Nigg, E. A. *Nature* **1997**, *386*, 789.

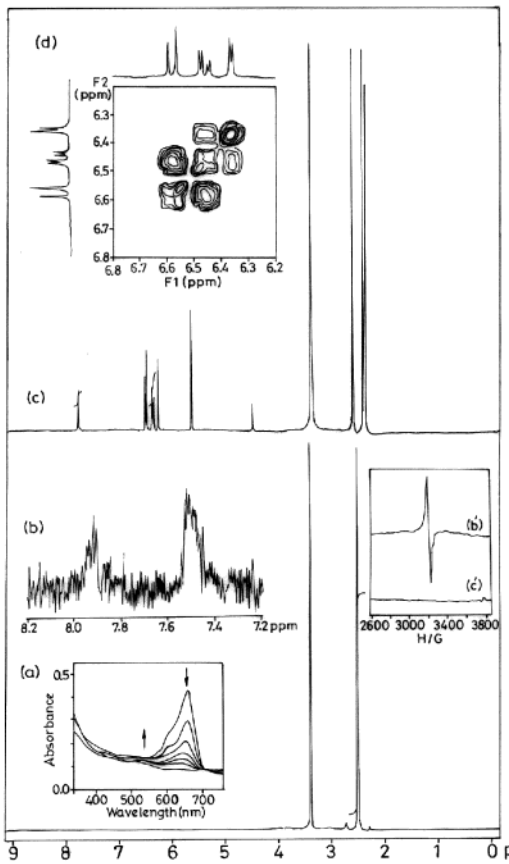


**Figure 1.** (a) Changes in the UV−vis spectra of **1** on reaction with dihydrogen in DMF. (b) and (b′) $^1$H NMR and ESR spectra, respectively, of **1**. (c) and (c′) $^1$H NMR and ESR spectra, respectively, of **1** after reaction with dihydrogen. (d) COSY spectrum of the aromatic region of the reduced form of **1** (see the Experimental Section) in DMSO-$d_6$.

bands of $Saf^+$ (in DMF at 535 nm, $\epsilon = 77\,300$) and $MB^+$ (in DMF at 665 nm, $\epsilon = 59\,000$), respectively. However, in **3** and **4** the band due to the cluster anion can be clearly seen at 620 nm. While $[NBu_4]_2[Pt_{12}(CO)_{24}]$ does not have an emission spectrum, **1** and **2** do. The spectra are very similar to those of ACl ($A^+ = MB^+$, $Saf^+$). An upward shift of only about 5 nm and no quenching are observed. This probably indicates very little perturbation of the electronic environments of the cations and no measurable interaction between the cluster and excited states of the dyes.

**(b) Reactions of 1−4 with Dihydrogen.** The reactions of **1**−**4** with dihydrogen have been carried out in DMF and DMSO and monitored spectroscopically. As shown in Figure 1a, the reaction of dihydrogen with **1** in DMF leads to the disappearance of the strong absorption band due to $MB^+$ at 665 nm. The color of the solution changes from deep blue to pale red, and the final pale red solution shows the absorption band of $[Pt_3(CO)_6]_3^{2-}$ at 560 nm. The spectral and color changes are consistent with the reactions shown by (e).

$$6MB^+ + 3[Pt_{12}(CO)_{24}]^{2-} + 7H_2 \rightarrow 6MBH + 4[Pt_9(CO)_{18}]^{2-} + 8H^+ \quad \text{(e)}$$

As already mentioned, the $^1$H NMR spectrum of **1** shows a very weak featureless signal in the aromatic region (see Figure 1b). Bulk magnetic susceptibility measurements at ambient temperatures show **1** to be diamagnetic (see the Experimental Section). However, in the ESR spectra of **1** both in solution and in the glass state (77 K), the presence of paramagnetic species is observed. An isotropic signal with $g = 2.002$ is seen (see Figure 1b′), indicating that the ESR active species is an organic radical. However, when dihydrogen is passed through the solution, the ESR signal disappears and sharp NMR signals emerge (see Figure 1c,c′,d).

In the solid state, the dye $MB^+$ is known to be ESR-active, due to the presence of small amounts of $MB^\bullet$ in L and H type defect sites.[8] At these defect sites two monocations, i.e., $MB^+$, react to give a dication ($MB^{2+}$) and $MB^\bullet$. In solution such reactions in defect sites are obviously not possible, and an alternative explanation for the formation of $MB^\bullet$ must be found.

Trace quantities of $MB^\bullet$ are probably formed in solution by reaction f and $MB^\bullet$ thus formed is trapped in the precipitated **1**. Interestingly, no ESR signal is

$$2MB^+ + 5[Pt_{12}(CO)_{24}]^{2-} \leftrightarrows 2MB^\bullet + 4[Pt_{15}(CO)_{30}]^{2-} \quad \text{(f)}$$

observed when $MB^+Cl^-$ is added to a DMF solution of $[Bu_4N]_2[Pt_{12}(CO)_{24}]$. This observation and the fact that no $[Pt_{15}(CO)_{30}]^{2-}$ could be seen in the dichloromethane solution of **1** by IR spectroscopy, suggest that equilibrium (f) lies mainly to the left. This is further supported by simple calculations based on previously measured $E_{p,a}$ values of the cluster[2] and the measured reduction potential of $MB^+$ (see later). These calculations show that the upper limit of the equilibrium constant of (f) is $10^{-20}$.

When dihydrogen is passed through the solution of **1**, $[Pt_{12}(CO)_{24}]^{2-}$ is converted into $[Pt_9(CO)_{18}]^{2-}$. The latter reduces $MB^\bullet$ according to reaction g, making the

$$2MB^\bullet + 4[Pt_9(CO)_{18}]^{2-} + 2H^+ \rightarrow 2MBH + 3[Pt_{12}(CO)_{24}]^{2-} \quad \text{(g)}$$

ESR signal disappear. It may be noted that combination of reactions b and g leads to catalytic reduction of $MB^\bullet$ to MBH by dihydrogen.

Although it is generally agreed that hydride addition takes place on N10, to the best of our knowledge the NMR ($^1$H) spectrum of MBH has not been reported in the literature.[9] A comparison of the NMR spectra of $MB^+Cl^-$ and the spectra obtained after the reaction of **1** with dihydrogen shows changes in the aromatic region and the emergence of three new peaks at $\delta$ 7.83, 5.73, and 4.6, which disappear on treatment with $D_2O$ (see Figure 1c and the Experimental Section). The stoichiometry of reaction e suggests that at the end of the reaction there are sufficient protons in the system that may protonate the "$NMe_2$" side chains of MBH. The three new signals are therefore assigned to the hydrogen of N10 in MBH and the acidic protons of mono- and diprotonated MBH. The coupling patterns of the aromatic protons in MBH have been studied by COSY experiments, and the results are fully consistent with

(8) Okuda, M.; Kowata, T.; Usui, Y.; Koizumi, M. *Bull. Chem. Soc. Jpn.* **1968**, *41*, 2274.
(9) Lee, S. K.; Mills, A. *Chem. Commun.* **2003**, 2366.

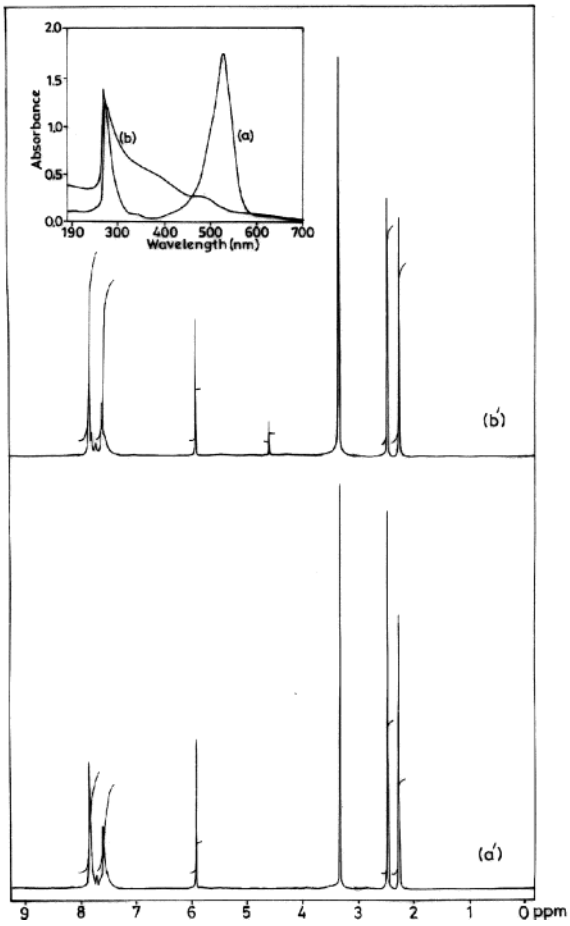


**Figure 2.** (a) and (a′) UV−vis and $^1$H NMR spectra, respectively, of **2** before reaction with dihydrogen in DMF. (b) and (b′) UV−vis and $^1$H NMR spectra, respectively, of **2** after reaction with dihydrogen in DMSO-$d_6$.

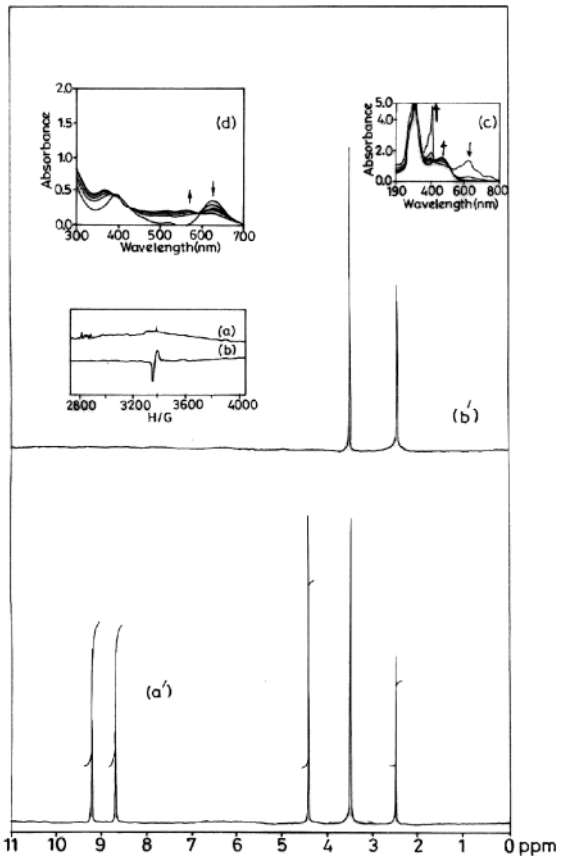


**Figure 3.** (a) and (a′) ESR and $^1$H NMR spectra, respectively, of **3** before reaction with dihydrogen in DMSO-$d_6$. (b) and (b′) ESR and $^1$H NMR spectra of respectively of **3** after reaction with dihydrogen. (c) and (d) Changes in UV−visible spectra of **3** on reaction with dihydrogen in DMF: (c) zero time spectrum recorded after formation of $MV^{\bullet+}$ in DMF; (d) zero time spectrum before reaction with dihydrogen and with a concentration of solution much less than that in (c).

selective hydride addition on N10 (see Experimental Section). Control experiments also established that a heterogeneous platinum catalyst such as Pt/C over-reduces $MB^+$. The reaction of $MB^+$ with dihydrogen, in the presence of Pt/C as the catalyst, leads to the disappearance of all the aromatic protons and the emergence of strong signals in the methylene region.

Unlike **1, 2**−**4** are found to be free of paramagnetic impurities and no ESR signals are seen. The reason that reactions analogous to (f) do not take place in the syntheses of **2**−**4** is probably due to more negative reduction potentials of $Saf^+$, $MV^{2+}$, and $BNA^+$ as compared to that of $MB^+$ (see later). As shown in Figure 2a, on reaction with dihydrogen, **2** loses the strong absorption band of $Saf^+$ at 535 nm. The color of the solution changes from deep red to almost colorless with a pinkish hue. The characteristic absorption of $[Pt_9(CO)_{18}]^{2-}$ in the bleached solution cannot be clearly seen because of the overlapping peaks of SafH.

However, the presence of $[Pt_9(CO)_{18}]^{2-}$ in the final solution is confirmed by IR bands at ∼2035 and ∼1850 $cm^{-1}$. NMR spectra of **2**, before reaction with dihydrogen, and $Saf^+Cl^-$ are identical. On reaction with dihydrogen one additional peak is observed at $\delta$ 4.63 (see Figure 2). This peak, which disappears on treatment with $D_2O$, is ascribed to the hydrogen of N10 in SafH. It may be noted that for MBH and SafH the chemical shifts of N10 protons, $\delta$ ∼4.63, are nearly the same. The overall reaction of **2** with dihydrogen is represented by (h).

$$6Saf^+ + 3[Pt_{12}(CO)_{24}]^{2-} + 7H_2 \rightarrow 6SafH + 4[Pt_9(CO)_{184}]^{2-} + 8H^+ \quad \text{(h)}$$

The reaction of **3** with dihydrogen leads to a change in color from light blue to purplish and disappearance of all the NMR signals. Simultaneously an ESR signal ($g_{isotropic}$(77 K) = 2.003) attributable to the radical cation $[MV^{\bullet}]^+$ appears. In reasonably concentrated solutions the color and UV−vis spectral signatures of $[Pt_9(CO)_{18}]^{2-}$ are masked by that of $[MV^{\bullet}]^+$ (in DMF at 608 nm, $\epsilon$ = 14 000). However, in dilute solutions the characteristic spectral changes associated with the conversion of $[Pt_{12}(CO)_{24}]^{2-}$ ($\epsilon$ = 23 000) to $[Pt_9(CO)_{18}]^{2-}$ ($\epsilon$ = 11 700) are observed (see Figure 3). Formation of $[MV^{\bullet}]^+$ is further confirmed by the fact that it can be reduced by hydrazine to give MV, which was characterized on the basis of its NMR spectrum. Since the reduction of $MV^{2+}$ by dihydrogen does not involve the addition of protons,

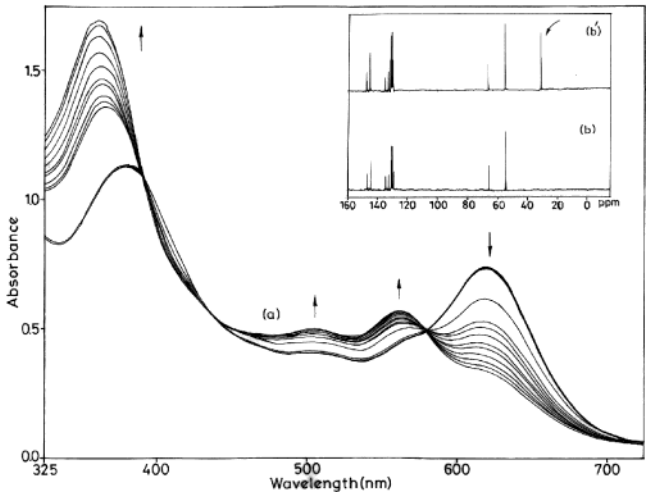


**Figure 4.** (a) Changes in the UV−vis spectra of **4** on reaction with dihydrogen in DMF. In the inset are shown changes in the $^{13}C$ NMR spectra of $BNA^+Cl^-$ on reaction with dihydrogen in a biphasic system with **2** as the catalyst. (b) and (b′) spectra of the $D_2O$ layer, before and after the reaction, respectively. The arrow indicates the formation of the new peak.

the above-mentioned observations are consistent with reaction i.

$$3[MV]^{2+} + 3[Pt_{12}(CO)_{24}]^{2-} + {}^5/_2H_2 \rightarrow 3[MV^{\bullet}]^+ + 5H^+ + 4[Pt_9(CO)_{18}]^{2-} \quad (i)$$

As already mentioned, a salt of $[Pt_{12}(CO)_{24}]^{2-}$ with $NAD^+$ as the countercation cannot be made, due to the latter's insolubility in organic solvents and also the presence of several potential ligands in its tail. The use of $BNA^+$ and analogous compounds as a model for $NAD^+$ in organic solvents is well documented.[6] Spectroscopic (UV−vis) monitoring of the reaction of **4** with dihydrogen shows the conversion of $[Pt_{12}(CO)_{24}]^{2-}$ to $[Pt_9(CO)_{18}]^{2-}$ (see Figure 4), but NMR monitoring does not show the formation of BNAH. Obviously $[Pt_9(CO)_{18}]^{2-}$ by itself can not reduce $BNA^+$, and the reaction of **4** with dihydrogen proceeds according to (j).

$$6[BNA]^+ + 3[Pt_3(CO)_6]_4^{2-} + H_2 \rightarrow 6[BNA]^+ + 4[Pt_3(CO)_6]_3^{2-} + 2H^+ \quad (j)$$

Reduction of $BNA^+$ in DMF through the intermediacy of SafH has also been explored. Thus, when a mixture of $BNA^+$ and **2** is reacted with dihydrogen, only trace quantities of BNAH and mainly unreacted $BNA^+$ are seen in the NMR ($^1H$) spectrum. The inability of $[Pt_9(CO)_{18}]^{2-}$ to reduce $BNA^+$ in DMF is probably due to the large negative reduction potential of $BNA^+$ in this solvent (see later).

As reported in our earlier communication, in a *biphasic* system, with **2** as the catalyst $BNA^+$ can be reduced by dihydrogen by combining reactions h and k.[4a] This

$$SafH + BNA^+ \rightarrow Saf^+ + BNAH \quad (k)$$

was concluded on the basis of UV−vis spectral changes of the aqueous layer. However, such evidence does not establish conclusively that hydride addition is fully selective toward the 4-position of the nicotinamide ring.

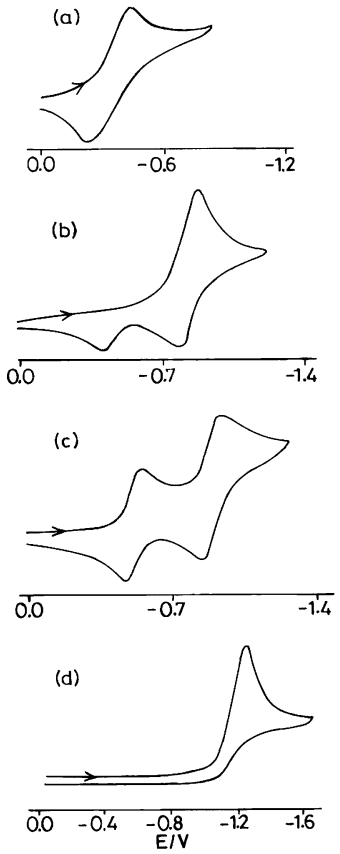


**Figure 5.** Cyclic voltammograms of $A^{n+}$ as chloride salts in DMF: $A^{n+} = MB^+$ (a), $Saf^+$ (b), $MV^{2+}$ (c), and $BNA^+$ (d).

**Table 1. Data on Reduction Potentials of $A^{n+}$**

| redox syst ($A^{n+}$) | $E°$ (V) in water and accompanying reacn | $E_{p,c}$ (V) in DMF and probable accompanying reacn |
|---|---|---|
| $MB^+$ | +0.011, $MB^+ + H^+ + 2e^-$ [11a] | −0.32, $MB^+ + 2e^-$ [a] |
| $Saf^+$ | −0.25, $Saf^+ + H^+ + 2e^-$ [11a] | −0.81, $Saf^+ + 2e^-$ [a] |
| $MV^{2+}$ | −0.45, $MV^{2+} + e^-$; −0.75, $MV^{\bullet+} + e^-$ [11b−d] | −0.5, $MV^{2+} + e^-$; −0.85, $MV^{\bullet+} + e^-$ [11e] |
| $BNA^+$ | −0.5, $BNA^+ + H^+ + 2e^-$ [a] | −1.22, $BNA^+ + 2e^-$ [a] |

[a] This work.

To establish the regioselectivity of the reaction, the $^{13}C$ NMR spectrum of the aqueous layer has been recorded (see Figure 4). A new peak at $\delta$ 30 ppm indicates that, in BNAH, the added hydride is located at the 4-position.

**(c) Cyclic Voltammetric Studies.** The redox properties of $[Pt_3(CO)_6]_3^{2-}$ in DMF using cyclic voltammetric technique have been reported recently.[2] Similar studies on the chloride salts of $A^{n+}$ ($n = 1$, $A = MB^+$, $Saf^+$, $BNA^+$; $n = 2$, $A = MV^{2+}$) have been carried out using a platinum working electrode and an SCE (saturated calomel electrode) as a reference. Representative voltammograms of $A^{n+}$ are shown in Figure 5, and the data are given in Table 1. $MB^+$, $Saf^+$, and $BNA^+$ exhibit one reductive response each in DMF. On scan reversal $MB^+$ shows one response, but two such responses are observed for $Saf^+$. However, an irreversible reductive response at a significantly higher negative potential is seen for $BNA^+$.

Expectedly, the electrochemical responses of $MV^{2+}$ are observed to be different from those of $MB^+$, $Saf^+$, $BNA^+$, displaying two well-defined reversible reductive couples. The cyclic voltammetric current height of the cathodic

response of $MB^+$ appears to be identical with that of the individual responses of $MV^{2+}$. On the other hand, the current heights corresponding to the voltamograms of $Saf^+$ and $BNA^+$ are found to be very similar and almost twice those observed for $MB^+$ and each of the responses associated with $MV^{2+}$.

In aqueous medium for $A^+$ the redox processes involve addition of one proton and two electrons, while for $A^{2+}$ only electrons are involved. In dry, distilled DMF, i.e., in the experimentally measured electrochemical responses, involvement of proton-donating impurities is highly unlikely.

The observed electrochemical responses of $MB^+$ and $MV^{2+}$ (Figure 5) may be tentatively assigned to one-electron addition to $MB^+$, resulting in $MB^\bullet$ and successive two one-electron additions to $MV^{2+}$, respectively. The assignment was made essentially on the basis of the following considerations: First, $MV^{2+}$ is a well-established electron acceptor center and, in accordance with its cationic charge, two successive one-electron reversible couples are seen. Second, the quasi-reversible reduction of $MB^+$ has a current height almost identical with that associated with each step of $MV^{2+}$. Third, the facile formation of $MB^\bullet$ is well documented in the literature, as already mentioned; in **1** trace quantities of $MB^\bullet$ can actually be detected by ESR.

In contrast, since the current heights of the cathodic waves for both $Saf^+$ and $BNA^+$ are almost identical and are twice that of $MB^+$ and each response of $MV^{2+}$, the observed cathodic responses for these two species ($Saf^+$ and $BNA^+$) may be tentatively considered as simultaneous two-electron-transfer processes. The electrode potentials of $A^{n+}$ in aqueous medium, with the exception of that of $BNA^+$, are available in the literature.[10] We have measured the cathodic response of $BNA^+$ in water, and all the data for comparison are shown in Table 1. It may be noted that $BNA^+$ has the highest negative reduction potential in both of the solvents. Accurate calculations of the thermodynamic feasibility of reaction l, in terms of $\Delta G$, requires the $\Delta G$ value of the $A^- + H^+ \rightarrow AH$ reaction and the redox potentials of the $A^+/A^-$ ($A^+ = Saf^+$, $BNA^+$) and $[Pt_9(CO)_{18}]^{2-}/[Pt_{12}(CO)_{24}]^{2-}$ couples. Assuming that $\Delta G$ values of the $A^- + H^+ \rightarrow AH$ reaction are not widely different for $Saf^+$ and $BNA^+$, the platinum cluster's ability to reduce $Saf^+$, but inability to do the same for $BNA^+$, is in accordance with their $E_{p,c}$ values. The difference in $E_{p,c}$ values of $Saf^+$ and $BNA^+$ in DMF is $\sim -0.4$ V, but in water it is $\sim -0.25$ V. From $E = (0.059/n) \log K$, a change of $-0.4$ V corresponds to a change in equilibrium constant of $\sim 10^{-13.5}$, while a change of $-0.25$ corresponds to a change of $\sim 10^{-8.5}$. In other words, the equilibrium constant for the reduction of $BNA^+$ in water is $10^5$ times more than that in DMF. This in turn may explain why SafH reduces $BNA^+$ in water (biphasic system), but the extent of reduction is considerably less in DMF.

$$A^+ + H^+ + 4[Pt_9(CO)_{18}]^{2-} \rightarrow 3[Pt_{12}(CO)_{24}]^{2-} + AH \quad (l)$$

**(d) Transport of $A^+$ across a Liquid Membrane.** Many model studies involving different types of liquid membranes have been reported in the literature.[12] Here, the transport of $A^+$ as AH ($A = MB^+$, $Saf^+$) from an aqueous layer through a layer of dichloromethane to another aqueous layer has been studied in a U-tube (see the Experimental Section). A dichloromethane layer separates the two aqueous layers, only one of which contains dissolved $A^+Cl^-$. As $A^+Cl^-$ is almost insoluble in dichloromethane, under nitrogen and in the absence of $[Bu_4N]_2[Pt_{12}(CO)_{24}]$ as the catalyst, there is no transport of $A^+Cl^-$ by diffusion through the organic layer. Control experiments also established that in the absence of a catalyst $A^+Cl^-$ could not be reduced by dihydrogen in a *monophasic* system consisting of either water or an organic solvent. However, in a *biphasic* system (water, dichloromethane), even in the absence of a catalyst, $A^+Cl^-$ could be partially reduced by dihydrogen. This is because in a biphasic system, as shown by (m), the equilibria are pushed to the right due

$$A^+Cl^-_{aq} + H_2 \rightleftharpoons HCl_{aq} + AH_{aq} \rightleftharpoons AH_{org} \quad (m)$$

to the greater solubility of AH in the organic phase, which in turn causes its part removal from the aqueous phase after its formation. In other words, the equilibria, as shown by (m), are pushed to the right. On exposure to dihydrogen, the reactions as shown by (n) are set up

$$A^+_{aq1} + H_2 \rightleftharpoons H^+_{aq1} + AH_{aq1} \rightleftharpoons AH_{org} \rightleftharpoons AH_{aq2} \quad (n)$$

and AH diffuses through dichloromethane from aqueous layer 1 (aq1) to aqueous layer 2 (aq2). The time-monitored concentration profiles of $A^+$ in the two aqueous layers are shown in Figure 6. The reduced dyes AH are known to undergo oxidation to give $A^+$ on exposure to air. The amount of transported AH could thus be measured by exposing the aqueous layers to oxygen and regenerating $A^+$. The rates of transport in the presence and absence of $[Bu_4N]_2[Pt_{12}(CO)_{24}]$ are shown. Clearly, in the presence of the cluster as the catalyst, the transport of $A^+$ as AH is much faster than that in the absence of the catalyst.

## Experimental Section

Unless stated otherwise, all operations were carried out by using standard Schlenk line techniques, with dry glassware, under an inert atmosphere. Solvents were dried, distilled under an atmosphere of prepurified argon atmosphere, and degassed prior to use. DMSO-$d_6$, DMF-$d_7$, and $ACl_n$ ($A = MB^+$, $Saf^+$, $MV^{2+}$, $n = 1, 2$) were purchased from Aldrich and used

(10) (a) Thanos, I.; Simon, H. *Angew. Chem., Int. Ed. Engl.* **1986**, *25*, 462. (b) Brad, A. J. *Science* **1980**, *207*, 139. (c) Toshima, N.; Takashi, T.; Hirai, H. *J. Macromol. Sci. Chem. A* **1988**, *25*, 669. (d) Lehn, J. M.; Sauvage, J. P. *Nouv. J. Chim.* **1977**, *1*, 449. (e) Kalyansundaram, K.; Kiwi, J.; Gratzel, M. *Helv. Chim. Acta* **1978**, *61*, 2720. (f) Harriman, A. *J. Chem. Soc., Chem. Commun.* **1990**, 24.

(11) (a) Mahler, H., R.; Cordes, E. H. *Biological Chemistry*, 2nd ed.; Harper and Row: New York, 1971; p 410. (b) Bird, C. L.; Kuhn, A. T. *Chem. Soc. Rev.* **1981**, *10*, 49. (c) Steckhan. E.; Kuwana, T. *Ber. Bunsen-Ges. Phys. Chem.* **1974**, *78*, 253. (d) Watanabe, T.; Honda, K. *J. Phys. Chem.* **1982**, *86*, 2617. (e) Monk, P. M. S. *The Viologens: Physicochemical Properties, Synthesis and Applications of the Salts of 4,4′-Bipyridine*; Wiley: New York, 1998.

(12) (a) Nakamura, H.; Linclau, B.; Curran, D. P. *J. Am. Chem. Soc.* **2001**, *123*, 10119, (b) Srividhya, J.; Gopinathan, M. S. *J. Phys. Chem. B* **2003**, *107*, 1438, (c) Wright, A. J.; Matthews, S. E.; Fischer, W. B.; Beer, P. D. *Chem. Eur. J.* **2001**, *7*, 3474. (d) Ohde, H.; Maeda, K.; Yoshida, Y.; Kihara, S. *Electrochim. Acta* **1998**, *44*, 23. (e) Sessler, J. L.; Ford, D. A.; Cyr, M. J.; Furuta, H. *J. Chem. Soc., Chem. Commun.* **1991**, *24*, 1733. (f) Meier, W.; Nardin, C.; Winterhalter, M. *Angew. Chem., Int. Ed.* **2000**, *39*, 4599. (g) Vincze, A.; Horvai, G.; Leermakers, F. A. M. *J. Phys. Chem.* **1996**, *100*, 8946.

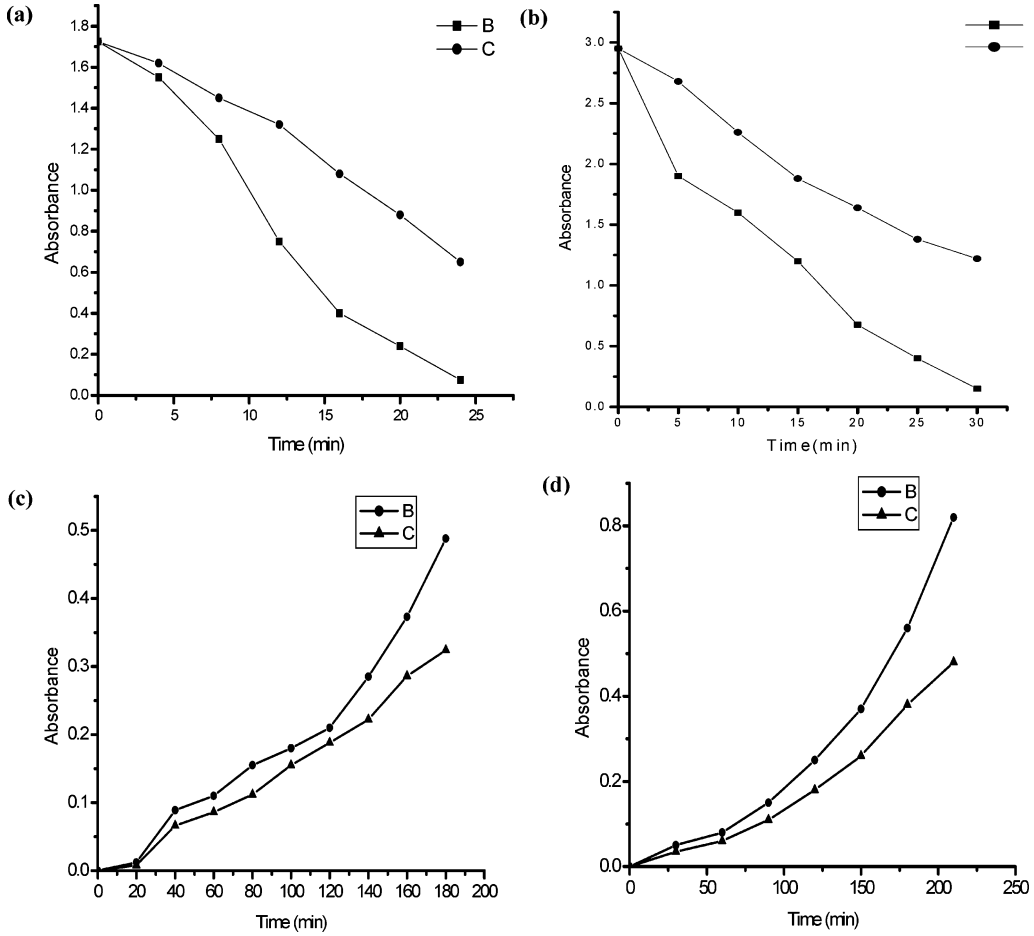


**Figure 6.** (a) and (b) catalyzed (indicated as B) and uncatalyzed (indicated as C) bleaching reaction progress for methylene blue and safranine O, respectively, at the left arm of the U-tube. (c) and (d) Facile autoxidation of the reduced dyes AH to give $A^+$ on exposure to air catalyzed (indicated as B) and uncatalyzed (indicated as C) for methylene blue and safranine O, respectively, at the right arm of the U-tube.



without further purification. $BNA^+Cl^-$ and $[Bu_4N]_2[Pt_{12}(CO)_{24}]$ were synthesized according to procedures reported in the literature.[1,6]

Infrared, UV−vis and fluorescence spectra were recorded on Nicolet Impact 400 and Shimadzu UV 2100 spectrometers. $^1H$ and $^{13}C$ NMR spectra have been recorded by using a Varian VXR-300S spectrometer. ESR studies have been carried out with a Varian Model 109C E-line X-band spectrometer with tetracyanoethylene radical as the calibrant. Magnetic susceptibility measurements were carried out on a Faraday balance at room temperature. Unless mentioned otherwise, all UV−vis, NMR, and ESR spectroscopic monitoring were carried out within the UV−vis cuvette or the NMR or ESR tube by using the standard rubber septa and cannula techniques used for air-sensitive compounds.

Cyclic voltammetric measurements were carried out under an atmosphere of dry argon using a Princeton Applied Research Model 273 A potentiostat/ galvanostat. A platinum working electrode (length 0.3 cm and diameter 0.5 mm), a platinum-wire auxiliary electrode, and a saturated calomel electrode (SCE) were used in a three-electrode configuration. $Bu_4N^+BF_4^-$ was used as the supporting electrolyte. The half-wave potential $E°_{298}$ was set equal to $0.5(E_{p,a} + E_{p,c})$, where $E_{p,a}$ and $E_{p,c}$ are the anodic and cathodic cyclic voltammetric peak potentials, respectively. For irreversible processes $E_{p,a}$ and $E_{p,c}$ were considered. All the cyclic voltammograms were recorded at a scan rate of 50 mV $s^{-1}$ unless otherwise mentioned.

**Synthesis of the $MB^+$ Salt of Platinum Carbonyl Cluster 1.** $Na_2PtCl_6·6H_2O$ (0.02 g, 0.0356 mmol) was added under a carbon monoxide atmosphere to a solution of anhydrous $CH_3COONa$ (0.004 g, 0.049 mmol) in 5 mL of methanol with constant stirring. After 24 h, the solution turned inkish blue, due to the formation of $[Pt_{12}(CO)_{24}]^{2-}$. A 3 mL methanol solution of 0.0018 g (0.0058 mmol) of methylene blue was added, and the mixture was stirred for 1 h. The resulting dark blue precipitate was filtered, washed with methanol, and dried under vacuum. Salts **2**−**4** were synthesized in a similar fashion.

**1**: $[MB]_2[Pt_{12}(CO)_{24}]$; yield 0.0092 g, 87%. Anal. Calcd for $C_{56}H_{36}N_6S_2O_{24}Pt_{12}$: C, 18.76; H, 1.00; N, 2.34; Pt, 65.37. Found: C, 18.82; H, 1.02; N, 2.36; Pt, 65.35. IR ($cm^{-1}$, KBr): $\nu_{CO}$ 2045, 1870. $^1H$ NMR (DMSO-$d_6$): broad, weak and featureless signal in the aromatic region. ESR: $g = 2.002$. Fluorescence (emission; $\lambda_{max}$/nm ($\epsilon/M^{-1}$ $cm^{-1}$) in DMF): 697 (59 000). $\chi = -5.32 \times 10^{-7}$ L/mol.

**2**: $[Saf]_2[Pt_{12}(CO)_{24}]$; yield 0.009 g, 84%. Anal. Calcd for $C_{64}H_{38}N_8O_{24}Pt_{12}$: C, 21.09; H, 1.04; N, 3.07; Pt, 64.25. Found: C, 21.3; H, 1.2; N, 3.1; Pt, 64.35. IR ($cm^{-1}$, KBr): $\nu_{CO}$ 2045, 1870. $^1H$ NMR (DMSO-$d_6$): $\delta$ 7.43−7.88 (m, 9H), 5.94 (s, 4H), 2.29 (s, 6H), Fluorescence (emission; $\lambda_{max}$/nm ($\epsilon/M^{-1}$ $cm^{-1}$) in DMF): 571 (73 000).

**3**: $[MV][Pt_{12}(CO)_{24}]$; yield 0.0089 g, 94%. Anal. Calcd for $C_{36}H_{14}N_2O_{24}Pt_{12}$: C, 13.5; H, 0.43; N, 0.875; Pt, 73.17. Found: C, 13.6; H, 0.46; N, 0.88; Pt, 73.2. IR ($cm^{-1}$, KBr): $\nu_{CO}$ 2045, 1870. $^1H$ NMR (DMSO-$d_6$): $\delta$ 9.2 (d, 4H), 8.7 (d, 4H), 4.5 (s, 6H).

**4**: $[BNA]_2[Pt_{12}(CO)_{24}]$; yield 0.0091 g, 89%. Anal. Calcd for $C_{50}H_{26}N_4O_{26}Pt_{12}$: C, 17.44; H, 0.756; N, 1.62; Pt, 68.07. Found: C, 17.4; H, 0.75; N, 1.65; Pt, 68.35. IR ($cm^{-1}$, KBr): $\nu_{CO}$ 2045, 1870. $^1H$ NMR (DMSO-$d_6$): $\delta$ 9.9 (s, 1H), 9.4 (d, 1H),

9.1 (d, 1H), 8.86 (s, 1H), 8.3 (dd, 1H), 8.2 (s, 1H), 7.64 (m, 2H), 7.48 (m, 3H), 5.95 (s, 2H).

**NMR Spectra of the Reaction Products of 1−4 with Dihydrogen.** A solution of **1** (0.0065 g, 0.0018 mmol) in DMSO-$d_6$ (1 mL) was placed in an NMR tube. $^1$H NMR (DMSO-$d_6$) signals for **1** were found to be weak and broad at $\delta$ 7.5 and 7.95, and the solution showed an ESR signal at $g = 2.002$. The DMSO-$d_6$ (1 mL) solution was reacted with dihydrogen, using standard techniques for handling air-sensitive compounds. The ESR signal disappeared, and the organic product was identified as MBH. $^1$H NMR (DMSO-$d_6$): $\delta$ 7.83 (s, 1H), 6.35 (d, 2H), 6.45 (dd, 2H, $J_{HH} = 7.8$ Hz, 2.6 Hz), 6.58 (d, 2H), 5.73 (1H), 4.6 (s, 1H), 2.73 (s, 12H). On treatment with $D_2O$ the signals $\delta$ 7.83, 5.73, and 4.6 disappear. COSY shows coupling of the aromatic protons, ortho coupling between $H_1$ and $H_2$ and meta coupling between $H_2$ and $H_4$. Same observations were made with DMF-$d_7$ as the NMR solvent, but the signals were less definitive due to background signals of DMF-$d_7$.

Reaction of **2** (0.0072 g, 0.00197 mmol) dissolved in 1 mL of DMSO-$d_6$ before and after reaction with dihydrogen was monitored by $^1$H NMR and ESR spectroscopy in a similar way. No signals were observed in the ESR measurements. After the reaction with dihydrogen the organic product, SafH, showed $\delta$ 7.43−7.88 (m, 9H), 5.94 (s, 4H), 4.63 (s, 1H), 2.29 (s, 6H) ($\delta$ 4.63 disappears on treatment with $D_2O$).

Reaction of **3** (0.0056 g, 0.00175 mmol) dissolved in 1 mL of DMSO-$d_6$ before and after reaction with dihydrogen was monitored by $^1$H NMR and ESR in a similar way. No signals were observed in ESR measurements before the reaction, and $^1$H NMR showed signals at $\delta$ 9.2 (d, 4H), 8.7 (d, 4H), 4.5 (s, 6H). The NMR signals disappeared after the reaction with dihydrogen. An ESR signal with $g_{isotropic} = 2.002$ is observed.

Reaction of **4** (0.012 g, 0.00349 mmol) dissolved in 1 mL of DMSO-$d_6$ before and after reaction with dihydrogen was monitored by $^1$H NMR and ESR in a similar way. No signals were observed in ESR before the reaction, and $^1$H NMR showed signals at $\delta$ 9.9 (s, 1H), 9.4 (d, 1H), 9.1 (d, 1H), 8.86 (s, 1H), 8.3 (dd, 1H), 8.2 (s, 1H), 7.64 (m, 2H), 7.48 (m, 3H), 5.95 (s, 2H). On $D_2O$ shaking signals at $\delta$ 8.86 (s, 1H) and 8.2 (s, 1H) disappear, which correspond to magnetically nonequivalent protons of the amide group present in **4**. After reaction of **4** with dihydrogen, the $^1$H NMR signals of $BNA^+$ remained unchanged. Reaction of a mixture of **2** (0.008 g, 0.00219 mmol) and $BNA^+Cl^-$ (0.011 g, 0.0442 mmol) was monitored by $^1$H NMR in a similar way. The organic products were identified as SafH, mainly unreacted $BNA^+$, and trace amounts of BNAH; $\delta$ 8.86 (s, 1H), 8.2 (s, 1H), 7.64 (m, 2H), 7.48 (m, 3H), 7.02 (s, 1H), 5.95 (s, 2H), 5.94 (d, 1H), 4.27 (m, 1H), 3.17 (d, 2H).

**Catalytic Reduction of $BNA^+Cl^-$ with Dihydrogen in a Biphasic System.** A $D_2O$ solution of $BNA^+Cl^-$ (0.0123 g, 0.0494 mmol in 2 mL) was layered over a 2 mL dichloromethane solution of **2** (0.0058 g, 0.001 59 mmol). Dihydrogen was passed through the mixture for 12 min, until the aqueous layer turned colorless and the organic layer turned green. An aliquot of the $D_2O$ layer was transferred to a NMR tube by cannula, and the $^1$H and $^{13}$C NMR spectra were recorded. Signals ($H^1$) were observed at $\delta$ 7.5 (m, 5H), 7.02 (s, 1H), 5.95 (s, 2H), 5.94 (d, 1H), 4.27 (m, 1H), and 3.17 (d, 2H). $^{13}$C signals for $BNA^+$ were found at $\delta$ 165 (s), 146.4 (s), 144.2 (s), 134.0 (s), 132.1 (s), 130.0 (s), 129.5 (s), 129.1 (s), 128.4 (s), 65 (s). and 53.8 (s, $CH_2Cl_2$ contamination), $^{13}$C NMR signals were observed for BNAH at $\delta$ 165 (s), 146.4 (s), 144.2 (s), 134.0 (s), 132.1 (s), 130.0 (s), 129.5 (s), 129.1 (s), 128.4 (s), 65 (s), 53.8 (s), and 30.0 (s). The new signal at $\delta$ 30 ppm is indicative of selective reduction at the 4-position of the pyridine ring.

**Transport of $A^+$/AH through a Liquid Membrane.** The U-tube was flushed with nitrogen, and a dichloromethane (30 mL) solution of $[Bu_4N]_2[Pt_{12}(CO)_{24}]$ (0.0025 g, 0.000 71 mmol) was placed in a U-tube (diameter 1.8 mm, length of vertical arms 170 mm, and length of horizontal part 60 mm) containing a small magnetic bead. An aqueous solution of $MB^+Cl^-$ (0.0015 g, 0.00047 mmol) in 30 mL of $H_2O$ was layered over the dichloromethane layer in the left arm, and only water (30 mL) was layered over the dichloromethane layer in the right arm. The dichloromethane layered was stirred for 10 min. No color change was observed. Measurement of $MB^+$ and $Saf^+$ by UV−visible spectrophotometry showed no formation and/or transport of MBH/SafH from the left to the right arm. Dihydrogen was passed through the dichloromethane layer for about 200 min, and care was taken not to allow any mixing of the two aqueous layers. The aqueous layer of the left arm was completely bleached in about 30 min. Time-monitored aliquots were taken from the right arm aqueous layer and were exposed to air for autoxidation of MBH. The absorbance of $MB^+$ thus formed was measured. The experiment with $Saf^+Cl^-$ (0.0015 g, 0.000 43 mmol) and similar experiments were performed under an atmosphere of hydrogen in the absence (control experiment) and also in the presence of $[Bu_4N]_2[Pt_{12}(CO)_{24}]$ (0.001 g, 0.000 29 mmol).

**Acknowledgment.** The help of Mr. H. Paul in the electrochemical measurements and financial support received from the Department of Science and Technology and Council for Scientific and Industrial Research, New Delhi, India, are gratefully acknowledged.

OM049833E